Title

Opposing Chromatin Signals Direct and Regulate the Activity of Lysine Demethylase 4C (KDM4C)*

Journal

Journal of Biological Chemistry, 291(12)

ISSN

0021-9258

Authors

Pack, Lindsey R
Yamamoto, Keith R
Fujimori, Danica Galonić

Publication Date

2016-03-01

DOI

10.1074/jbc.m115.696864

THE JOURNAL OF BIOLOGICAL CHEMISTRY VOL. 291, NO. 12, pp. 6060–6070, March 18, 2016

Opposing Chromatin Signals Direct and Regulate the Activity of Lysine Demethylase 4C (KDM4C)*

Received for publication, October 6, 2015, and in revised form, January 7, 2016 Published, JBC Papers in Press, January 8, 2016, DOI 10.1074/jbc.M115.696864

Lindsey R. Pack[‡§], **Keith R. Yamamoto**[‡1], **and Danica Galonić Fujimori**[‡¶2]

From the [‡]*Department of Cellular and Molecular Pharmacology, the* [§]*Tetrad Graduate Program, and the* [¶]*Department of Pharmaceutical Chemistry, University of California, San Francisco, California 94158*

Histone H3 lysine 4 trimethylation (H3K4me3) and histone H3 lysine 9 trimethylation (H3K9me3) are epigenetic marks with opposing roles in transcription regulation. Whereas colocalization of these modifications is generally excluded in the genome, how this preclusion is established remains poorly understood. Lysine demethylase 4C (KDM4C), an H3K9me3 demethylase, localizes predominantly to H3K4me3-containing promoters through its hybrid tandem tudor domain (TTD) (1, 2), providing a model for how these modifications might be excluded. We quantitatively investigated the contribution of the TTD to the catalysis of H3K9me3 demethylation by KDM4C and demonstrated that TTD-mediated recognition of H3K4me3 stimulates demethylation of H3K9me3 in *cis* on peptide and mononucleosome substrates. Our findings support a multivalent interaction mechanism, by which an activating mark, H3K4me3, recruits and stimulates KDM4C to remove the repressive H3K9me3 mark, thus facilitating exclusion. In addition, our work suggests that differential TTD binding properties across the KDM4 demethylase family may differentiate their targets in the genome.

Post-translational modifications of histone proteins regulate chromatin structure and accessibility and act as part of the chromatin scaffold to control many nuclear processes. Lysine methylation, one of the most functionally diverse histone modifications, has a regulatory role in a range of processes, including heterochromatin formation, transcriptional regulation, and DNA repair (3, 4). Both the extent of methylation (mono-, di-, or trimethylation) and the position of the lysine within the histone tail determine the functional effect of the modification by recruiting different effector proteins. Of particular interest are two modifications with opposing effects on transcription, histone H3 lysine 9 trimethylation (H3K9me3)[3] and histone H3 lysine 4 trimethylation (H3K4me3). H3K9me3 is a major component of silent heterochromatin and in euchromatic promoters is generally associated with repressed transcription (5–9). In contrast, H3K4me3 is found at euchromatic promoters and correlates with active transcription (10–13). These chromatin modifications have critical and opposing roles in regulating gene expression, and colocalization of H3K9me3 and H3K4me3 on the same nucleosome is generally excluded in the genome (14, 15). Although this exclusivity must be tightly controlled, the mechanisms that preclude colocalization of these histone marks are poorly understood.

The spatial and temporal localization of histone lysine methylation are regulated by the opposing activities of histone modifying enzymes. Histone lysine methyltransferases are "writers" that deposit methyl groups on lysines, whereas histone lysine demethylases are "erasers" that remove the methylation. In principle, the exclusion of colocalized modifications could be explained by a methyltransferase that functions at H3K9 only in the absence of H3K4me3 (or vice versa). Indeed, several H3K9 methyltransferases are partially inhibited by H3K4me3 (16, 17), and MLL2, a H3K4 methyltransferase, is similarly inhibited by H3K9me3 (18). Mutual exclusivity could additionally be achieved by demethylases that are selective for H3K9me3 in the presence of H3K4me3 (or vice versa). This selectivity could be achieved through recognition of the opposing modification by "reader" domains embedded within the demethylase. A few instances of reader domains affecting the activity of a demethylase have been identified. For example, the activity of KDM5A toward its H3K4me3 substrate is stimulated in *trans* by recognition of unmodified H3 by a plant homeodomain (PHD) reader domain (19). In addition, the PHDs of two KDM7 demethylases, PHF8 and KDM7A, recognize H3K4me3 with different effects on their activities, activating and inhibiting H3K9me2 demethylation, respectively (20). This latter example demonstrates a role for demethylases in integrating H3K4 and H3K9 methylation states.

KDM4 demethylases, an important and conserved family of H3K9me3 erasers, present an excellent model for probing the role of demethylases in excluding the colocalization of H3K9me3 and H3K4me3. The KDM4 histone demethylases act on H3K9me3/me2 and, in some cases, H3K36me3/me2 (21–26). In vertebrates, this family is composed of five family mem-

* This work is supported by a National Science Foundation Graduate Research Fellowship (to L. R. P.), National Institutes of Health (NIH) Grant R01 CA020535 (to K. R. Y.), and NIH Grant R01 GM114044, Searle Scholar, and University of California San Francisco Nina Ireland Program for Lung Health awards (to D. G. F.). The authors declare that they have no conflict of interest with the contents of this article.

[1] To whom correspondence may be addressed: Dept. of Cellular and Molecular Pharmacology, University of California San Francisco, S572D Genentech Hall, 600 16th St., San Francisco, CA 94143. Tel.: 415-476-8445; Fax: 415-514-4112; E-mail: Yamamoto@ucsf.edu.

[2] To whom correspondence may be addressed: Dept. of Cellular and Molecular Pharmacology, University of California San Francisco, N572E Genentech Hall, 600 16th St., San Francisco, CA 94143. Tel.: 415-514-0147; E-mail: Danica.Fujimori@ucsf.edu.

[3] The abbreviations used are: H3K9me3, histone H3 lysine 9 trimethylation; H3K4, H3K9, and H3K36, histone H3 lysine 4, 9, and 36, respectively; H4K20, histone H4 lysine 20; me0, me1, me2, me3, un-, mono-, di-, trimethylated, respectively; KDM4 and -7, lysine demethylase 4 and 7, respectively; KDM4C cat, KDM4C catalytic domain; KDM4C fl, full-length KDM4C; TTD, tandem tudor domain; PHD, plant homeodomain; TEV, tobacco etch virus protease; FP, fluorescence polarization; TCEP, tris(2-carboxyethyl)phosphine; aa, amino acids; NTA, nitrilotriacetic acid; GUIM, Grace's unsupplemented insect medium; Tricine, *N*-tris(hydroxymethyl)methylglycine.

bers, KDM4A-E (25, 27), but despite their shared histone methylation substrates (21–26), it appears that at least KDM4B and KDM4C function at distinct genomic loci (1). Whereas KDM4B occupancy is more evenly distributed across different genomic regions, KDM4C localizes predominantly to H3K4me3-containing promoter regions (1, 2). Although the similarity between their catalytic domains is unlikely to generate specificity (25, 28), KDM4A-C have several reader domains, including two PHDs of unknown function and a hybrid tandem tudor domain (TTD) (Fig. 1*A*), which may act as specificity determinants. Previous work has shown that the TTD of KDM4A binds to H3K4me3 and H4K20me3, and the TTD of KDM4B binds methylated H4K20 (29–32). However, only recently have the binding properties of the KDM4C TTD been qualitatively assessed to bind methylated H3K4 (2), intriguingly connecting this H3K9 demethylase to H3K4me3. Indeed, an intact TTD is required for the recruitment of KDM4C to H3K4me3-modified genomic loci (2). We were intrigued by the possibility that, in addition to the recruitment function, recognition of H3K4me3 by the TTD modulates KDM4C catalytic efficiency toward its H3K9me3 substrate. We therefore set out to quantitatively investigate the affinity of the KDM4C TTD for H3K4me3 and determine whether recognition of this mark impacts the enzymatic activity of KDM4C.

Experimental Procedures

Cloning KDM4C Construct—KDM4C tandem tudor domain (KDM4C TTD) (amino acids (aa) 877–991) was cloned into the pETARA vector (gift from the W. Lim laboratory) downstream of the DNA sequence encoding the glutathione *S*-transferase (GST) tag and tobacco etch virus protease (TEV) recognition site using standard cloning methods. The KDM4C catalytic domain (KDM4C cat) (aa 1–352) was similarly cloned into the pBH4 His_6 vector (gift from the W. Lim laboratory) downstream of the sequence encoding the His_6 tag and TEV recognition site. A construct fusing the catalytic domain and TTD (KDM4C mini) (aa 1–352 5× glycine-serine linker 877–991) was generated using the Gibson method (33) to introduce a 5× glycine-serine linker and the TTD sequence (aa 877–991) into the pBH4 His_6 KDM4C cat construct. KDM4C full-length (KDM4C fl) was cloned into the pFastBac-HTB vector downstream of the sequence encoding the His_6 and TEV recognition site using standard cloning methods. All constructs were generated using the sequence for human KDM4C. Point mutants were introduced by site-directed mutagenesis.

Expression and Purification of KDM4C Constructs—KDM4C TTD, KDM4C cat, and KDM4C mini constructs were expressed in Rosetta pLysS *Escherichia coli* grown in Terrific Broth medium. Cultures were grown at 37 °C to an $A_{600} = 0.6$, cooled to 18 °C, and induced with 300 μM isopropyl β-D-1-thiogalactopyranoside for 20 h. Cells were harvested by centrifugation at 3,500 rpm for 15 min. Cell pellets containing KDM4C TTD were lysed in 50 mM HEPES, pH 7.5, 500 mM NaCl, 0.5 mM phenylmethylsulfonyl fluoride (PMSF) by sonication. Cell debris was removed by subsequent centrifugation at 35,000 rpm for 45 min at 4 °C. KDM4C TTD was purified using glutathione-Sepharose 4B resin (GE Healthcare) and washed with 50 mM HEPES, pH 7.5, 500 mM NaCl. KDM4C TTD was eluted with 50 mM HEPES, pH 7.5, 100 mM NaCl, 30 mM reduced glutathione. Following elution, proteins were dialyzed in 50 mM HEPES, pH 7.5, 100 mM NaCl. If necessary, KDM4C TTD constructs were purified by subsequent size exclusion chromatography (S75 26/60). For isothermal titration calorimetry, the GST tag of the KDM4C TTD was cleaved by TEV while dialyzing in 50 mM HEPES, pH 7.5, 50 mM NaCl. The TTD was subsequently purified by size exclusion chromatography (S75 26/60). KDM4C cat and KDM4C mini cell pellets were lysed in 50 mM HEPES, pH 8.0, 500 mM NaCl, 20 mM imidazole, and 0.5 mM PMSF by a microfluidizer. Lysate was clarified as for KDM4C TTD. KDM4C cat and KDM4C mini were purified using Qiagen Ni-NTA resin and washed with 50 mM HEPES, pH 8.0, 500 mM NaCl, and 20 mM imidazole. Constructs were eluted using 50 mM HEPES, pH 8.0, 500 mM NaCl, 250 mM imidazole, and 0.5 mM TCEP. The His_6 tags were cleaved by TEV for 4 h at 4 °C while dialyzed in 50 mM HEPES, pH 8.0, 500 mM NaCl, 0.5 mM TCEP. Following cleavage, the protein was incubated with Ni-NTA resin, and the flow-through was collected. KDM4C cat was further purified by size exclusion chromatography in 50 mM HEPES, pH 8.0, 500 mM NaCl (S75 26/60). KDM4C mini was further purified by size exclusion chromatography in 50 mM HEPES, pH 8.0, 150 mM NaCl (S200 26/60).

Bacmid for KDM4C fl was made following Invitrogen's Bac to Bac Expression System guidelines. Recombinant bacmids were isolated and transfected into Sf21 cells to generate recombinant baculovirus. For transfections, 0.9×10^6 cells were seeded in one well of a 6-well dish in Sf 900 II SFM medium containing 50 units/ml penicillin and 50 μg/ml streptomycin. While cells attached, 2–5 μg of bacmid diluted in 100 μl of Grace's unsupplemented insect medium (GUIM) was mixed with 6 μl of Cellfectin reagent diluted in 100 μl of GUIM. This Bacmid/Cellfectin reagent mixture was incubated at room temperature for 25–40 min. Once cells were attached, they were rinsed with GUIM and treated with the Bacmid/Cellfectin mixture diluted in 1 ml of GUIM. Cells were incubated for 5 h at 27 °C. Following incubation, the GUIM was replaced with Sf 900 II SFM containing 50 units/ml penicillin and 50 μg/ml streptomycin. Transfections were incubated for 3–4 days at 27 °C or until signs of viral infection were observed. The virus-containing supernatant was collected, centrifuged, and sterile filtered to obtain the P1 viral stock. P2 virus was generated by infecting cells in log phase at $\sim 1.5 \times 10^6$ cells/ml with 1 ml of P1 virus per 20 ml of cells. Cells were grown for 55 h at 27 °C, and the supernatant was collected, centrifuged, and sterile filtered to obtain the P2 virus. This viral amplification process was repeated, infecting with P2 virus to obtain the P3 virus, which was used for the large scale expression of KDM4C fl. For expression, 1.2 liters of cells growing in log phase at $\sim 1.5 \times 10^6$ cells/ml were infected with P3 virus (25 ml/1.2 liter of cells). Cells were allowed to grow at 27 °C for 55 h and then were harvested by centrifugation at 3,000 rpm for 15 min.

Sf21 pellets were lysed in 50 mM HEPES, pH 8, 500 mM NaCl, 20 mM imidazole, 0.5 mM PMSF, 2 $\mu g\ ml^{-1}$ aprotinin, 3 $\mu g\ ml^{-1}$ pepstatin, and 3 $\mu g\ ml^{-1}$ leupeptin. Cells were lysed using a microfluidizer and centrifuged at 35,000 rpm for 45 min at 4 °C. KDM4C fl was purified using Qiagen's Ni-NTA resin. Resin was washed with 50 mM HEPES, pH 8, 500 mM NaCl, 20 mM imid-

azole and with 50 mM HEPES, pH 8, 150 mM NaCl, and 20 mM imidazole. KDM4C fl was eluted using 50 mM HEPES, pH 8, 150 mM NaCl, 250 mM imidazole, and 0.5 mM TCEP. Following elution, TEV cleavage of the His_6 tag was performed while dialyzing in 50 mM HEPES, pH 8, 150 mM NaCl, 0.5 mM TCEP at 4 °C for 4 h. KDM4C fl was further purified by size exclusion chromatography (S200 26/60) in 50 mM HEPES, pH 8, 150 mM NaCl. Proteins were at least 95% pure of other contaminants. Protein concentrations were determined by a Bradford assay.

Fluorescence Polarization Assays—KDM4C TTD binding studies were performed by either direct or competition-based fluorescence polarization (FP) assays. Fluorescent H3K4me3 (aa 1–18) and H4K20me3 (aa 16–25) peptides (Genescript), containing a 5-carboxyfluorescein on either a natural or unnatural C-terminal lysine, were used at 10 nM in the direct FP assay. Assays were performed in 50 mM HEPES, pH 7.5, 50 mM NaCl, and 0.01% Tween 20, incubated for 30 min at room temperature, and FP was measured using a Molecular Devices SpectraMax M5e microplate reader with an excitation wavelength of 492 nm and emission wavelength of 517 nm. For direct FP binding assays, KDM4C TTD constructs were serially diluted and incubated with the fluorescent peptide. For FP competition assays, 2 μM KDM4C TTD was incubated with 10 nM H3K4me3 fluorescent peptide and competitor peptides of varying concentrations. Competitor peptides were unlabeled H3K4me0, H3K4me1, H3K4me2, H3K4me3, and H3K4me3K9me3 (aa 1–18) (Genescript). FP direct binding assays were fit as described previously (34), and competition assays were fit using the following equation.

$$FP_{obs} = \frac{K_i(FP_{max}[TTD] + FP_{min}K_d) + FP_{min}K_d[I]}{K_i(K_d + [TTD]) + K_d[I]} \quad \text{(Eq. 1)}$$

Isothermal Titration Calorimetry Assays—KDM4C TTD lacking the GST tag was dialyzed into 50 mM HEPES, pH 7.5, 50 mM NaCl, and H3K4me3 (aa 1–10) and H4K20me3 (aa 16–25) were resuspended in the same buffer. The experiment was performed using a MicroCal VP-ITC calorimeter (GE Healthcare) at 25 °C. H3K4me3 or H4K20me3 peptide (500 μM) was titrated from the syringe into a 50 μM cell solution of KDM4C TTD. The heat of dilution, measured from titration of peptide into isothermal titration calorimetry buffer, was subtracted from the binding data. Calorimetric parameters were calculated by fitting to a one-site binding model using Origen 7.0 software.

Peptide Demethylation—Kinetic analysis of KDM4C peptide demethylation was performed using an enzyme-coupled assay that follows the production of formaldehyde (35). A master mix containing α-ketoglutarate (500 μM), ascorbic acid (500 μM), $Fe(NH_4)_2(SO_4)_2$ (50 μM), NAD^+ (2 mM), and formaldehyde dehydrogenase (0.05 units) was mixed in 50 mM HEPES, pH 7.7, 50 mM NaCl with KDM4C constructs of interest. KDM4C constructs were used at 1 μM for all kinetic studies with the exception of KDM4C fl with H3K4me3K9me3, which was used at 0.2 μM to better estimate the K_m. Assays were initiated with the addition of various concentrations of H3K9me3 and H3K4me3K9me3 (aa 1–15) (Genscript). In addition to H3K9me3 peptides, KDM4C fl assays were performed with H3K9me2 and H3K4me3K9me2 (aa 1–15) peptides (CPC Scientific). Fluorescence was monitored every 20 s for 30 min at room temperature on a Molecular Devices SpectraMax M5e microplate reader using 340-nm excitation and 460-nm emission wavelengths. The coupled assay was also used to compare KDM4C fl demethylation of H3K9me3, H3K4me3K9me3, and H3K9me3 with H3K4me3 in *trans*. For these assays, 1 μM KDM4C fl was used in the master mix described above with or without H3K4me3 (100 μM) provided in *trans*. Reactions were initiated with the addition of either H3K9me3 or H3K4me3K9me3 substrate to a final concentration of 1.56 μM. All reactions were analyzed using NADH standard curves to convert fluorescence to concentration of product formed. Initial rates were determined using the first 3 min of the reaction, plotted against the substrate concentration, and fit with the Michaelis-Menten equation to determine the kinetic parameters.

Demethylation of peptides was alternatively analyzed by matrix-assisted laser desorption/ionization time-of-flight (MALDI-TOF) mass spectrometry. We performed the assays in 50 mM HEPES, pH 7.7, 50 mM NaCl with α-ketoglutarate (500 μM), ascorbic acid (500 μM), and $Fe(NH_4)_2(SO_4)_2$ (50 μM) and incubated KDM4C fl (1 μM) with H3K9me3 or H3K4me3K9me3 (aa 1–15) peptides (2 μM). Demethylation was initiated by the introduction of peptide, and time points were collected over 30 min at room temperature before samples were quenched by EDTA (final concentration 5 mM). Samples were desalted by C18-ZipTip (Millipore) and diluted 1:10 in H_2O with 0.01% trifluoroacetic acid (TFA). The extent of demethylation and product distribution was analyzed by MALDI-TOF mass spectrometry (Shimazu) using α-cyano-4-hydroxycinnaminic acid as the matrix.

Methylated Nucleosome Reconstitution—We used a previously described His_6-Smt3-H3(15–136 A15C) construct to express and purify the H3(15–136 A15C) fragment for native chemical ligation (19). Expression and initial purification of the histone from the inclusion bodies were performed as described previously (36). Following extraction from the inclusion bodies, the His_6-Smt3-H3 (15–136 A15C) was precipitated by dialysis in H_2O with 5 mM β-mercaptoethanol. Precipitated pellet was resuspended in 9 M urea and subsequently diluted in 50 mM HEPES, pH 6.8, 150 mM HEPES, 150 mM L-Arg, 10 mM L-Cys, bringing the final concentration of urea to 2 M and protein to 0.25 mg/ml. An approximately 1:10 mass/mass ratio of Senp1-SUMO(419–644) protease to protein was added to samples and incubated at 4 °C overnight. The cleaved histone was passed over Qiagen Ni-NTA resin three times, and the flow-through was dialyzed in 1% acetic acid. Histone was lyophilized and further purified by semipreparative Luna C-18 (250 × 21.20 mm × 10 μm) (Phenomenex) reverse phase HPLC using a 35–55% acetonitrile with 0.1% TFA gradient for 1 h at 15 ml/min. Native chemical ligation was performed as described previously (37), using H3K9me3-(*S*-benzyl) and H3K4me3K9me3-(*S*-benzyl) 14-mers (CPC Scientific). Ligation was purified as above, using a 35–55% acetonitrile with 0.1% TFA gradient for 2 h at 15 ml/min. Following purification of ligated product, desulfurization of Cys-15 to the native Ala was performed via a free radical-based approach as described previously (37, 38). Desulfurized histone was dialyzed in H_2O with 5 mM β-mercaptoethanol. Except for H3K9me3 and H3K4me3K9me3 his-

tones, all other *Xenopus laevis* histones were recombinantly expressed and purified using standard procedures (36).

The 147-bp standard 601 sequence DNA was produced by PCR and was used for all nucleosome assemblies (39, 40), with the exception of nucleosomes used for the pull-down assay. DNA for the pull-down assay contained 5′-biotin, and the sequence was a slight variation of the 601 sequence, containing a PstI site 16 bp from the 5′-end. Octamers and nucleosomes were assembled using previously published procedures (36).

Quantitative Western Blotting—Mononucleosome demethylase assays were performed in 50 mM HEPES, pH 7.7, 50 mM NaCl with α-ketoglutarate (500 μM), ascorbic acid (500 μM), and $Fe(NH_4)_2(SO_4)_2$ (50 μM) at room temperature. Concentrations of KDM4C fl and KDM4C mini were optimized for the given nucleosome substrates (1.5 μM for H3K9me3 and 0.5 μM for H3K4me3K9me3 nucleosomes). Assays were initiated by the addition of either H3K9me3 or H3K4me3K9me3 mononucleosomes (0.125 μM). Time points were quenched in 1:1 6× protein loading buffer to 500 mM EDTA, pH 8.0 (70 mM final), and boiled. Samples were run on 4–20% Tris-Tricine Bio-Rad gels for 30 min at 200 V. Gels were transferred onto nitrocellulose membrane using the Bio-Rad Trans-Blot SD semidry transfer system for 1 h at 24 V. Western blots were blocked for 1 h using LI-COR Odyssey blocking buffer and then incubated overnight at 4 °C with rabbit anti-H3K9me3 (Abcam ab8898; 1:1000) and rabbit anti-H4 (Active Motif 39-269; 1:1000) in 1:1 PBS/Odyssey blocking buffer containing 0.02% Tween 20. Membranes were incubated with IRDye 680LT goat anti-rabbit secondary antibody (LI-COR 926-68021; 1:20,000) in 1:1 PBS/Odyssey blocking buffer containing 0.02% Tween 20 for 1 h at room temperature. Membranes were visualized using LI-COR. Samples were shown to be in the linear range of the primary antibodies. No cross-reactivity was observed for the anti-H3K9me3.

Westerns blots were quantified using LI-COR Odyssey application software. H3K9me3 fluorescent signal was normalized to that of histone H4. Demethylation was normalized to time = 0 min, plotted against time, and analyzed as described previously (41). k_{cat}/K_m was estimated by dividing the k_{obs} by the enzyme concentration.

Mononucleosome Pull-down Assay—1 μg of either unmodified mononucleosomes, H3K4me3-containing nucleosomes, biotinylated BSA, or molar equivalent of biotinylated 601 sequence was immobilized on 10 μl of streptavidin resin (M-280 Dynabeads, Invitrogen) in 50 mM HEPES, pH 7.5, 150 mM NaCl, 0.01% Tween 20, and 0.1 mg/ml BSA (PD buffer) for 30 min at 4 °C. The resin was washed two times with PD buffer, and the immobilized nucleosomes were incubated with 10 μl of 0.5 μM KDM4C in PD buffer for 30 min at 4 °C. Following incubation, the resin was washed two times with PD buffer. Beads were boiled in 20 μl of SDS loading buffer, and Western blots were used to analyze the pull-down. We used a rabbit anti-KDM4C antibody raised in rabbit against GST-tagged KDM4C aa 361–436 to detect KDM4C fl (Covance). Samples were within the linear range of the antibody.

Results

Recognition of H3K4me3 by the KDM4C TTD—A qualitative pull-down previously demonstrated that the KDM4C TTD specifically recognized H3K4me3 (2). We sought to validate and extend this observation using a quantitative approach to further explore the affinity and specificity of the KDM4C TTD. We determined its binding properties toward H3K4me3 and H4K20me3, modifications known to be recognized by the KDM4A TTD (29–31). We purified GST-tagged KDM4C TTD and characterized its binding to fluorescent histone peptides with different modifications through FP assays. We found that the KDM4C TTD recognizes H3K4me3 but not H4K20me3 (Fig. 1*B*). This result was validated in an isothermal titration calorimetry assay, excluding the possibility that lack of binding was due to interference by the fluorophore (Fig. 2). The K_d of the KDM4C TTD toward H3K4me3 was 2–4 μM, consistent with affinities observed for other methylation readers (42–44), and the stoichiometry observed was ~1:1. Moreover, this recognition of H3K4me3 was recapitulated using a full-length KDM4C protein construct (KDM4C fl), which bound the peptide with an affinity of 5 μM (Fig. 1*B*).

To determine the impact of the H3K4 methylation state on the KDM4C TTD affinity, we performed FP competition assays in which the binding of the TTD to the fluorescently labeled H3K4me3 peptide was competed with unlabeled H3K4me0, H3K4me1, H3K4me2, and H3K4me3 peptides. We found a preference for the highest methylation state (H3K4me3) and progressive reductions in affinity with the loss of methyl groups (me3 > me2 > me1 > me0) (Fig. 1, *C* and *D*), consistent with the recognition of methylated lysine by an aromatic cage in the TTD peptide interface (30, 31). This aromatic cage recognition was further validated by a point mutation (Y953A) in the KDM4C TTD, which was chosen based on sequence alignment and structural studies with the KDM4A TTD (30, 31). We confirmed through FP assays that the Y953A mutation abrogated H3K4me3 binding (Fig. 1*B*). Additionally, we asked whether H3K9me3, one of the demethylation substrates of KDM4C, had any effect on the ability of the KDM4C TTD to bind H3K4me3. By comparing the affinities of H3K4me3 alone with peptides containing both H3K4me3 and H3K9me3, we found that the KDM4C TTD binds these peptides equivalently and is not influenced by the trimethylation of H3K9 (Fig. 1, *C* and *D*).

H3K4me3 Stimulates KDM4C Demethylation of H3K9 Methylated Peptides—The observation that the KDM4C TTD specifically recognizes H3K4me3 propelled us to investigate the effect this modification might have on the enzymatic activity of KDM4C. We compared KDM4C fl-catalyzed demethylation of H3K9me3 and H3K9me2 peptides with the corresponding substrates containing both H3K4 and H3K9 methylation: H3K4me3K9me3 and H3K4me3K9me2. Demethylation was monitored by a formaldehyde release assay (35). We observed that H3K4me3 stimulated the catalytic efficiency (k_{cat}/K_m) of H3K9me3 and H3K9me2 demethylation by 9- and 24-fold, respectively (Fig. 3*A* and Table 1). In addition to improving the demethylation of both substrates, the presence of Lys-4 trimethylation narrows the difference in catalytic efficiency between tri- and dimethylated H3K9 to <2-fold.

To gain an insight into the manner in which demethylation is stimulated in the presence of H3K4me3, we compared two individual kinetic parameters: k_{cat}, a measure of the maximum rate of demethylation, and K_m, a measure of the relative affinity toward

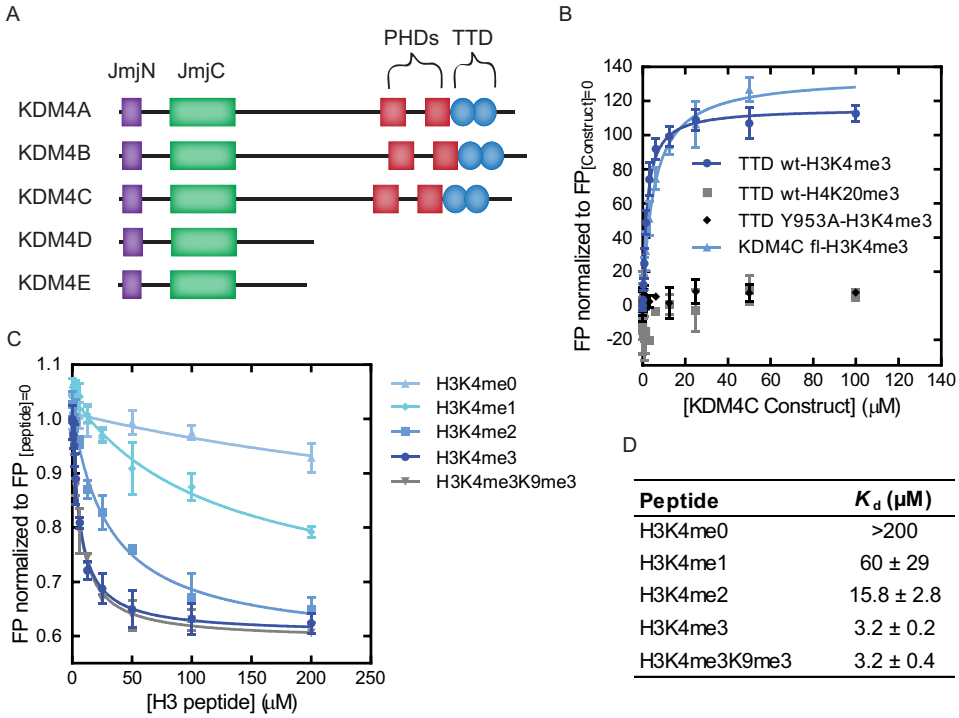

D

Peptide	K_d (μM)
H3K4me0	>200
H3K4me1	60 ± 29
H3K4me2	15.8 ± 2.8
H3K4me3	3.2 ± 0.2
H3K4me3K9me3	3.2 ± 0.4

FIGURE 1. **Recognition of H3K4me3 by the KDM4C TTD.** *A*, KDM4 family domain architecture as predicted by SMART sequence analyzer. Shown are Jumonji domain N (*JmjN*), Jumonji domain C (*JmjC*), PHDs, and the TTD. *B*, FP-based analysis of binding between KDM4C constructs (KDM4C fl or KDM4C TTD, either wild type (*wt*) or containing the Y953A mutation) and fluorescently labeled H3K4me3 (18-mer) and H4K20me3 (11-mer) peptides. Data points for KDM4C fl extend only to 50 μM due to the difficulty in expressing large amounts of this protein. *C*, FP competition assay comparing the KDM4C TTD binding to H3 peptides with different H3K4 methylation states or H3K4me3K9me3 modifications. All peptides were 18-mers. *D*, dissociation constants derived from *C*. *Error bars* ($n \geq 3$), S.E.

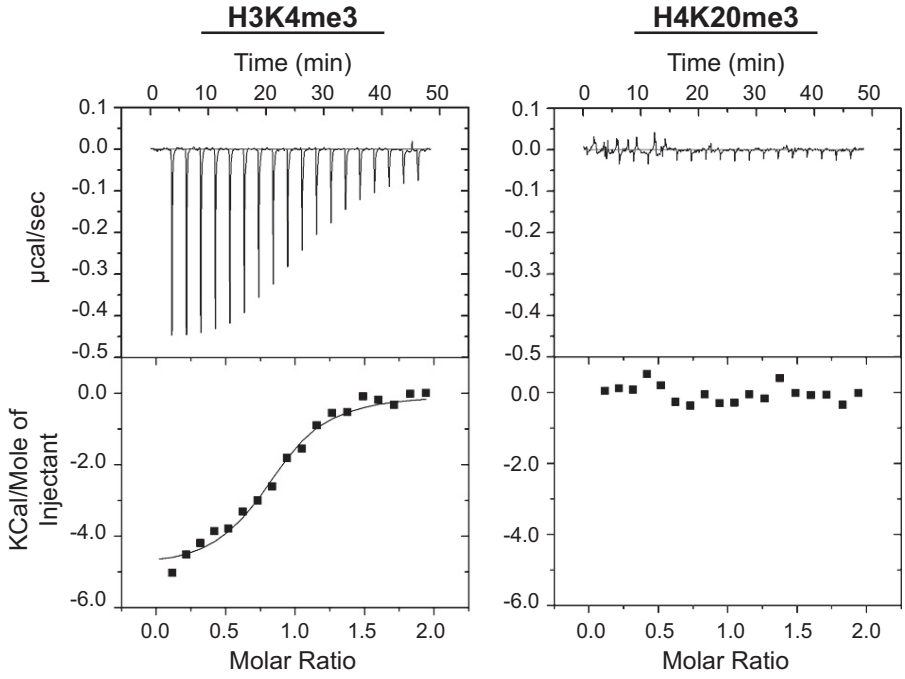

FIGURE 2. **Isothermal titration calorimetry analysis of KDM4C TTD binding.** *Top panels*, data obtained from automatic 2-μl injections of either 500 μM H3K4me3 (10-mer) or H4K20me3 (11-mer) into a cell containing KDM4C TTD lacking the GST tag (50 μM). *Bottom panels*, integrated curve with experimental points and best fit curve for a one-binding site model. Interaction of KDM4C TTD and the H3K4me3 was determined to have an $n = 0.80 \pm 0.02$ and $K_d = 3.2 \pm 0.1$ from the average of two independent ITC measurements.

the substrate. We found that H3K4me3 decreases the K_m of H3K9me3 and H3K9me2 demethylation by 16- and 27-fold, respectively, with the k_{cat} of H3K9me3 decreasing less than 2-fold and virtually unchanged for H3K9me2 (Table 1). Thus, the effect of H3K4me3 on H3K9 demethylation is predominantly through a significant increase in the affinity between the substrate and KDM4C fl, as represented by a decrease in the K_m. Together, these results indicate that H3K4me3 stimulates the catalytic efficiency of

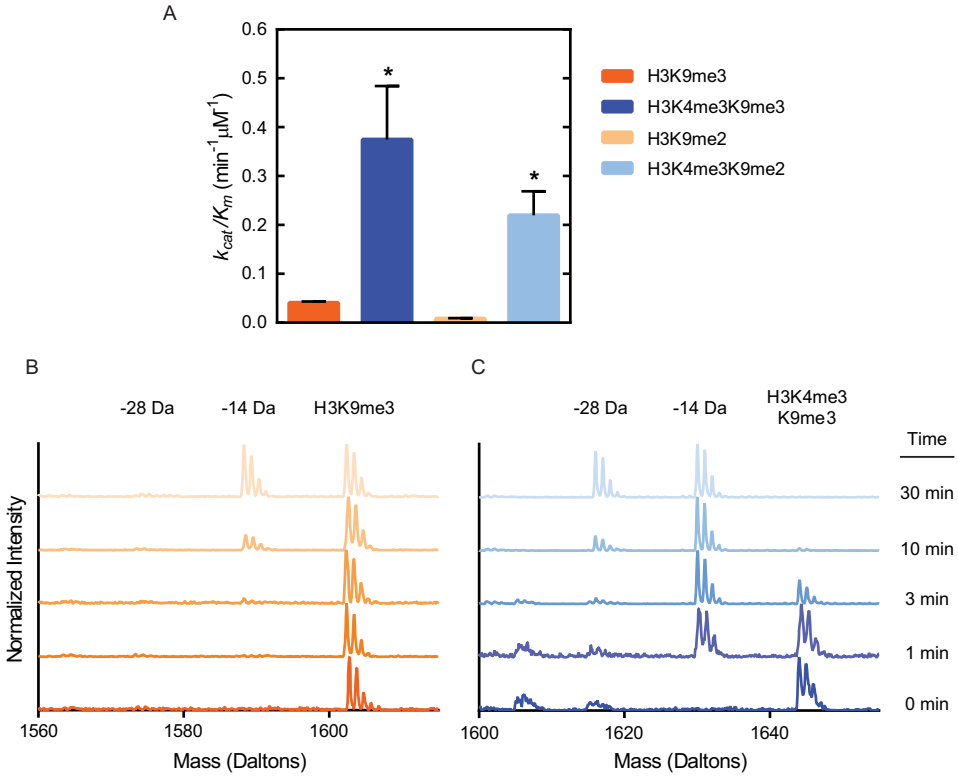

FIGURE 3. **H3K4me3 stimulates KDM4C demethylation of H3K9 methylated peptides.** *A*, comparison of k_{cat}/K_m values derived from Michaelis-Menten analysis of KDM4C fl demethylation of H3K9me3, H3K4me3K9me3, H3K9me2, and H3K4me3K9me2 15-mer peptides. *Error bars* ($n \geq 3$), S.E. *B*, MALDI-TOF analysis of H3K9me3 15-mer demethylation by KDM4C fl over a time course from 0 to 30 min. *C*, MALDI-TOF analysis of H3K4me3K9me3 15-mer demethylation by KDM4C fl over a time course from 0 to 30 min.

TABLE 1

Kinetic parameters of KDM4C fl demethylation of peptide substrates

Shown are Michelis-Menten-derived kinetic parameters of KDM4C fl activity on H3K9me3, H3K4me3K9me3, H3K9me2, and H3K4me3K9me2. Errors ($n \geq 3$) represent S.E.

Substrate	KDM4C fl		
	k_{cat}	K_m	k_{cat}/K_m
	min^{-1}	μM	min^{-1} μM^{-1}
H3K9me3	0.79 ± 0.01	19.4 ± 1.2	0.041 ± 0.003
H3K4me3K9me3	0.45 ± 0.01	1.2 ± 0.4	0.38 ± 0.11
H3K9me2	0.137 ± 0.003	16.0 ± 1.6	0.009 ± 0.001
H3K4me3K9me2	0.132 ± 0.003	0.6 ± 0.1	0.22 ± 0.05

KDM4C by enhancing the interaction of the demethylase with methylated H3K9 peptides.

Additionally, we analyzed KDM4C fl demethylation of H3K9me3 and H3K4me3K9me3 peptides using MALDI-TOF mass spectrometry as a more direct method to monitor demethylation. We found a similar stimulation of H3K9 demethylation in the presence of H3K4me3 (Fig. 3, *B* and *C*). This method also allowed us to compare the product distribution throughout the time course of demethylation. We observed a faster accumulation of H3K9me2 in the presence of H3K4me3, followed by an accumulation of H3K9me1 toward the end of the time course, distinct from the products observed for peptides containing H3K9me3 alone (Fig. 3, *B* and *C*). These results are consistent with a model in which H3K4me3 provides enhanced affinity and thus enzymatic efficiency toward methylated H3K9 peptides.

The TTD Is Necessary and Sufficient for H3K4me3-mediated Binding Enhancement—Based on our results from the KDM4C TTD peptide binding studies, we hypothesized that the TTD is critical to the stimulation of KDM4C enzymatic activity by H3K4me3, but whether this domain is necessary or sufficient was unknown. We compared four KDM4C constructs to elucidate the mechanism of stimulation by H3K4me3: (i) KDM4C fl; (ii) the catalytic domain alone (KDM4C cat); (iii) KDM4C full-length with the Y953A mutation that precludes binding of the TTD to H3K4me3 (KDM4C Y953A) (Fig. 1*B*); and (iv) a construct in which the catalytic domain is linked to the TTD by a short glycine-serine linker (*GS-linker*) (KDM4C mini) (Fig. 4*A*). We determined the ability of these four constructs to demethylate H3K9me3 and H3K4me3K9me3 peptides. Unlike KDM4C fl, the enzymatic activities of KDM4C cat and KDM4C Y953A were unchanged by the presence of H3K4me3 (Fig. 4*B* and Table 2). This result demonstrated that a functional TTD is necessary for the stimulatory effect of H3K4me3. Moreover, we observed that H3K4me3 had no effect on KDM4C cat catalysis, indicating that recognition and demethylation of H3K9me3 by the catalytic domain is not directly affected by H3K4me3 (Table 2). In contrast, we found that the demethylation of H3K9me3 by KDM4C mini was stimulated 6-fold by H3K4me3 (Fig. 4*B* and Table 2). Similar to KDM4C fl, this stimulation resulted from a decrease in the K_m, in this case by 7-fold (Table 2). The observed stimulation of KDM4C mini, although diminished relative to that observed in the KDM4C fl, indicates that the presence of the TTD is sufficient for recognition of H3K4me3.

We next investigated how H3K4me3 stimulates demethylation by KDM4C. We considered two potential modes for this stimulation: (i) in *cis*, by which KDM4C engages both H3K4me3 and H3K9me3 on a single histone tail; (ii) in *trans*,

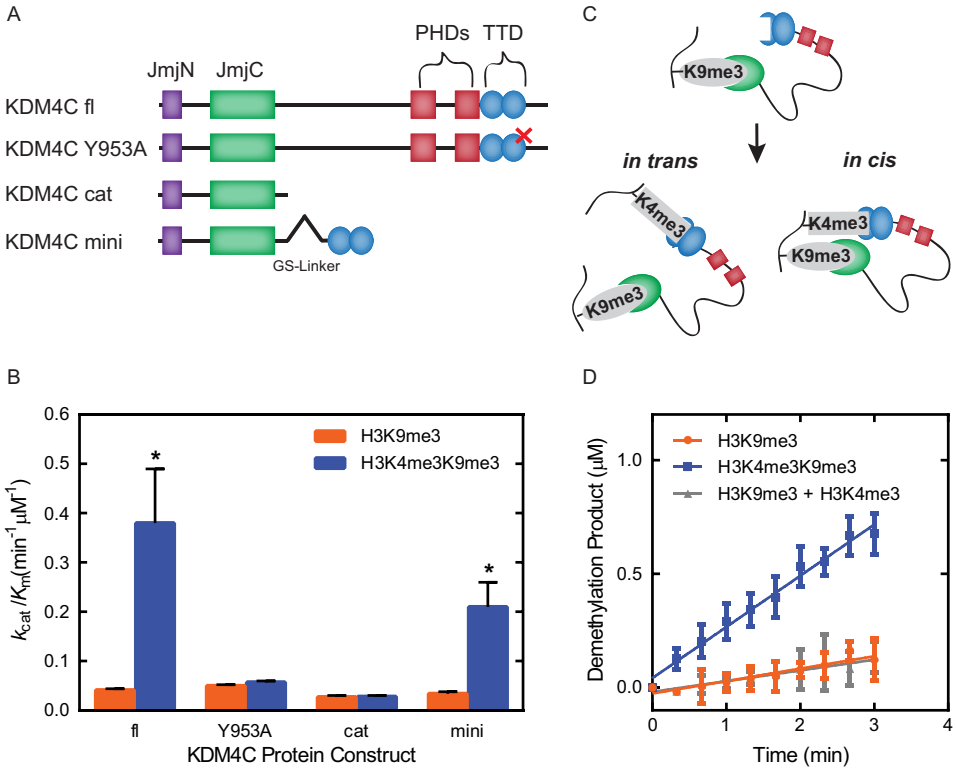

FIGURE 4. **TTD-mediated H3K4me3 recognition stimulates demethylation.** *A*, domain architecture of the constructs used to investigate the mechanism of H3K4me3 stimulation. *B*, comparison of k_{cat}/K_m derived from Michaelis-Menten analysis of demethylation of H3K9me3 and H3K4me3K9me3 15-mer peptides catalyzed by KDM4C fl, KDM4C Y953A, KDM4C cat, or KDM4C mini. *Error bars* ($n \geq 3$), S.E. *C*, schematic of potential modes of stimulation of KDM4C fl by H3K4me3. H3K4me3 peptide could stimulate H3K9me3 either in *trans* or in *cis*. *D*, comparison of observed rates of demethylation by KDM4C fl toward H3K9me3 (*orange*), H3K4me3K9me3 (*blue*), and H3K9me3 in the presence of saturating H3K4me3 provided in *trans* (*gray*).

whereby the TTD and catalytic domain interact with H3K4me3 and H3K9me3, respectively, on different histone tails (Fig. 4*C*). To distinguish these modes, we compared the rates of KDM4C fl demethylation of peptides in three reactions: (i) a H3K9me3 peptide alone; (ii) a peptide containing both H3K4me3 and H3K9me3; and (iii) a H3K9me3 peptide in the presence of an additional peptide containing only H3K4me3 at a saturating concentration. We found that H3K4me3 only stimulated demethylation when in *cis* to the H3K9me3 substrate (Fig. 4*D*). Thus, we conclude that H3K4me3 stimulates KDM4C when in *cis* to the substrate modification, H3K9me3.

Demethylation and Binding Properties of KDM4C on Methylated Mononucleosomes—Given our finding that H3K4me3 stimulates KDM4C-catalyzed H3K9me3 demethylation of peptides containing both marks, we sought to determine whether the same effect could be observed on a more complex substrate, the mononucleosome. We produced histones containing the H3K9me3 or H3K4me3K9me3 modifications by native chemical ligation of modified histone H3 N-terminal peptides to the rest of the histone H3 fragment that was recombinantly expressed (Fig. 5*A*) (37, 38). These generated H3 histones were then assembled into octamers and subsequently nucleosomes (36), which we validated (Fig. 5*A*), and used in demethylation assays under single turnover, subsaturating enzyme conditions. Demethylation was analyzed by quantitative Western blotting (Fig. 5*A*), and the catalytic efficiency (k_{cat}/K_m) was estimated by dividing the observed rate by the enzyme concentration. We found that H3K4me3 stimulated the estimated catalytic efficiency (k_{cat}/K_m) of KDM4C fl- and KDM4C mini-catalyzed demethylation of H3K9me3 by 3- and 6-fold, respectively (Fig. 5*B*). These findings demonstrate that H3K4me3 stimulates demethylation on mononucleosomes as well as peptides.

We further investigated whether an enhancement in binding was responsible for the H3K4me3 stimulation on nucleosomes, consistent with the mechanism identified on peptides. We compared the binding preference of KDM4C fl toward unmodified and H3K4me3 nucleosomes using an *in vitro* pull-down assay (45). We found that KDM4C fl preferentially binds to H3K4me3-containing nucleosomes compared with unmodified nucleosomes (Fig. 5*C*). This preference was consistent with the stimulation in demethylation of H3K9me3-containing nucleosomes in the presence of H3K4me3. These results indicate that in the context of recombinant mononucleosomes, H3K4me3 stimulates demethylation through enhancing the affinity of KDM4C for the substrate in a mechanism similar to that observed with the peptide studies.

Discussion

H3K4me3 Stimulates KDM4C-mediated Demethylation by Enhancing Substrate Affinity—Our quantitative studies revealed that the KDM4C TTD recognizes methylated H3K4, with a preference for the trimethylated form. The presence of H3K4me3 in *cis* significantly stimulated the demethylation of methylated H3K9 both on peptides and mononucleosomes. Our peptide studies indicated that recognition of H3K4me3 by the TTD was necessary and sufficient for this stimulation. To

TABLE 2

Kinetic parameters of demethylation of peptide substrates by KDM4C constructs

Shown are Michaelis-Menten-derived kinetic parameters for demethylation of H3K9me3 and H3K4me3K9me3 by KDM4C constructs. Errors ($n \geq 3$) represent S.E.

Construct	H3K9me3			H3K4me3K9me3		
	k_{cat}	K_m	k_{cat}/K_m	k_{cat}	K_m	k_{cat}/K_m
	min^{-1}	μM	$min^{-1}\ \mu M^{-1}$	min^{-1}	μM	$min^{-1}\ \mu M^{-1}$
KDM4C fl	0.79 ± 0.01	19.4 ± 1.2	0.041 ± 0.003	0.45 ± 0.01	1.2 ± 0.4	0.38 ± 0.11
KDM4C Y953A	1.30 ± 0.01	25.9 ± 1.0	0.050 ± 0.002	1.15 ± 0.01	20.1 ± 0.8	0.057 ± 0.003
KDM4C cat	0.85 ± 0.02	31.0 ± 2.7	0.027 ± 0.003	0.81 ± 0.01	29.0 ± 1.3	0.028 ± 0.002
KDM4C mini	0.99 ± 0.02	28.7 ± 2.6	0.034 ± 0.004	0.84 ± 0.03	4.0 ± 0.8	0.21 ± 0.05

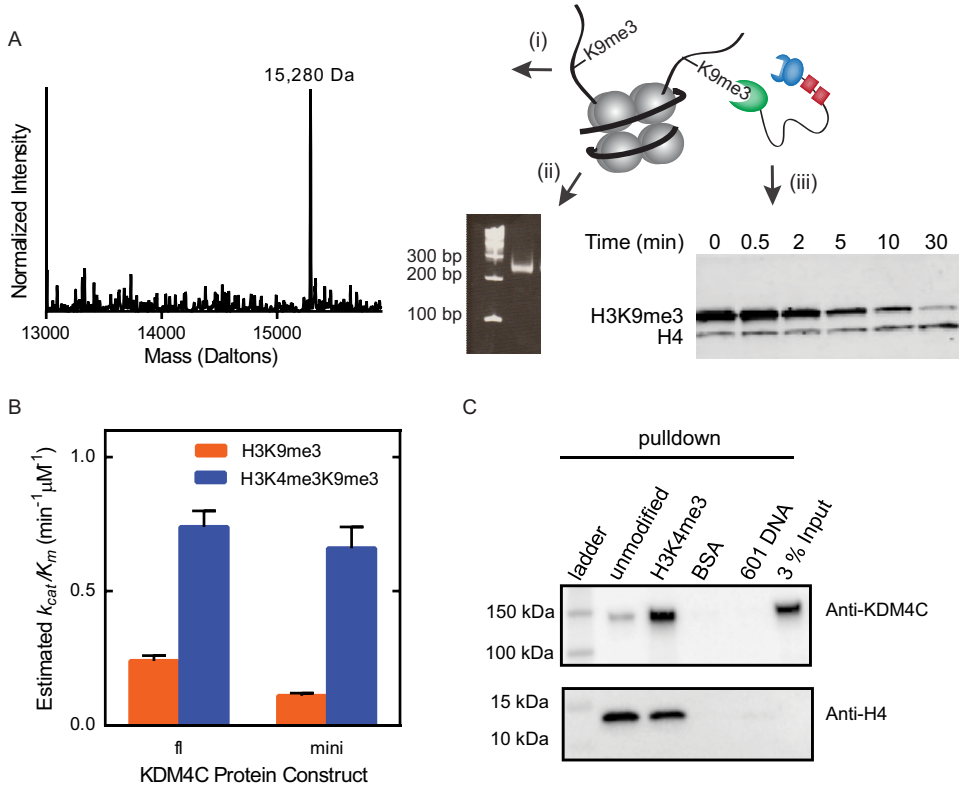

FIGURE 5. **H3K4me3 stimulation of KDM4C on mononucleosomes.** *A*, assessment of mononucleosome quality. *i*, representative liquid chromatography mass spectrometry trace of H3K9me3-modified histones produced by native chemical ligation and desulfurization. *ii*, DNA polyacrylamide gel (5% acrylamide, 0.5× TBE) demonstrating that the mononucleosomes are fully assembled and lack free DNA at 147 bp. *iii*, representative quantitative Western blot of a KDM4C fl demethylation time course of H3K9me3-containing mononucleosomes. Similar validation was performed for unmodified and H3K4me3K9me3-containing mononucleosomes. *B*, comparison of approximate k_{cat}/K_m for demethylation of H3K9me3 and H3K4me3K9me3 nucleosomes by KDM4C fl and KDM4C mini. *Error bars* ($n = 2$), S.E. *C*, comparison of binding preference of KDM4C fl as determined by *in vitro* pull-down assay. Purified KDM4C fl was incubated with streptavidin beads coated with biotinylated unmodified nucleosomes, biotinylated H3K4me3-containing nucleosomes, biotinylated BSA, and biotinylated DNA. After incubation, the beads were washed, and the bound protein was eluted by boiling the beads in SDS buffer. Western blots were used to assess the amount of KDM4C fl bound in each condition.

our knowledge, this study is the first to identify a modulation of the activity of KDM4C due to the function of its reader domain. We propose a multivalent interaction model (Fig. 6), in which two linked modifications are engaged by the protein through multiple domain interactions to increase the affinity and specificity toward the dual-modified substrate (46, 47). This model is supported by the following evidence: (i) KDM4C fl was stimulated by H3K4me3 through a binding enhancement both on peptides and mononucleosomes (Table 1 and Fig. 5*C*), and (ii) stimulation required that H3K4me3 reside in *cis* to H3K9me3 (Fig. 4*D*). In the proposed mechanistic model, the TTD recognition of H3K4me3 enhances the interaction with the substrate, stimulating demethylation by increasing the affinity of KDM4C toward methylated H3K9.

Our peptide results differ from a previous report, which observed that H3K4me3 equivalently affects demethylation in both the catalytic domain and the full-length KDM4C, both by an approximately 2-fold enhancement (48). In contrast, we observe H3K4me3 stimulation only for the KDM4C fl construct, by ~10-fold. The source of the differences between the two studies remains unclear but could be due to differences in assay conditions, peptide lengths, or the presence of affinity tags. Our model is strengthened by our demonstration that the Y953A point mutation in the TTD abrogates the stimulation by H3K4me3 and that the artificial tethering of the TTD is sufficient to stimulate H3K9me3 demethylation in the presence of H3K4me3. The proposed reader domain recognition enhances KDM4C binding, activity, and specificity, offering additional modes of regulation.

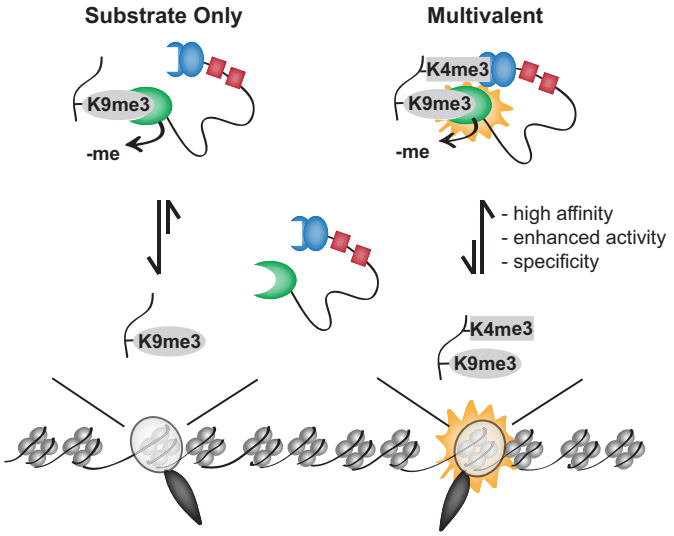

FIGURE 6. **Model for stimulation of the enzymatic activity of KDM4C by H3K4me3.** H3K4me3 recognition by the TTD stimulates KDM4C demethylation by enhancing the affinity of KDM4C toward its substrate. This multivalent interaction can provide specificity for substrates containing both methylated H3K4 and H3K9.

Complex Interactions with the Mononucleosome—Whereas demethylation of mononucleosome substrates is stimulated by the presence of H3K4me3, net enhancement of KDM4C fl activity was lower than the effect measured on peptides (Figs. 3*A* and 5*B*). Consistent with this observation, KDM4C fl distinguishes unmodified and H3K4me3-containing peptides to a greater extent than the respective mononucleosomes. The dampened stimulation could be attributed to the increased affinity of KDM4C fl for the more complex nucleosome substrate, irrespective of the presence of H3K4me3. Whereas *in vitro*, this difference may be attributed to additional contacts that the demethylase might make with the nucleosome beyond the interaction of the TTD with H3K4me3, the *in vivo* chromatin context is likely to influence how nucleosomes are presented to KDM4C. Moreover, in some regions of the nucleosome packaged genome, histone tails may be the most accessible components of chromatin. In any case, our results indicate that beyond the role of H3K4me3 in the recruitment of KDM4C, this modification also stimulates the enzymatic efficiency of the demethylase toward its H3K9me3 substrate.

Regulatory Potential of KDM4C Interactions—Our finding that KDM4C activity is regulated by H3K4me3-dependent TTD interactions opens the possibility that additional post-translational modifications in the N-terminal region of the H3 tail (49) could modulate TTD binding and thus the catalytic activity. In addition, it is possible that the TTD interaction with H3K4me3 might similarly regulate the removal of another known KDM4C substrate, methylated H3K36 (21, 22, 25). Given the significantly higher K_m of H3K36me3 compared with H3K9me3 (35), it is conceivable that the proposed multivalency mechanism may more strongly enhance demethylation of methylated H3K36. In this context, H3K4me3 could prohibit the spreading of H3K36me3 into the promoter from intragenic regions where it is generally localized (9, 15, 50). Moreover, the clear regulatory role established for the KDM4C TTD should motivate studies of the KDM4C PHD domains, potential reader domains of unknown function. Finally, in addition to chromatin modifications, KDM4C could be regulated through protein-protein interactions with other chromatin factors or complexes, consistent with the observation that the activity of *Drosophila* KDM4A is stimulated by HP1 (51). These hypotheses remain to be tested.

Specialized Reader Domains—The KDM4 family of demethylases expanded from predominantly one demethylase to five in the vertebrate lineages (25, 27), yet all five of these enzymes act on trimethylated H3K9, a seemingly redundant function (21–26). Recent *in vivo* studies demonstrate that KDM4B and KDM4C have overlapping but also distinct targets (1), indicating mechanisms that generate specificity. Our study demonstrates that the differences in the function of the TTD reader domains, present in KDM4A-C, may provide genomic specificity. Whereas the KDM4A TTD recognizes both H3K4me3 and H4K20me3 (29–31), and the KDM4B TTD binds methylated H4K20 (32), we and Pederson *et al.* (2) have shown that the KDM4C TTD is specialized to recognize only methylated H3K4 (Figs. 1*B* and 2). This specialization of the KDM4C TTD recognition and, importantly, its effect on KDM4C H3K9me3 demethylation revealed in this study might create specificity for a narrower subset of targets. This specificity is particularly important given that the concentration of KDM4C is probably limiting relative to its substrate. Thus, our findings highlight both specialization of KDM4C from other KDM4 family members and a mechanism that contributes to its specificity for certain substrates.

The functional specialization of the TTD and its effect on KDM4C substrate specificity are reminiscent of Src homology 2 and 3 domains, recognition modules present in a number of signaling proteins, including kinases. In addition to their roles in substrate recognition, Src homology 2 and 3 domains regulate enzymatic activity through a multitude of mechanisms, including multivalent interactions and allostery (52, 53). In analogy to these signaling modules, the TTDs of the KDM4 demethylases participate both in substrate recognition and modulation of enzymatic activity. These observations suggest parallels in regulation achieved by auxiliary domains across diverse enzyme families.

Mechanism for Establishing or Maintaining an Active State—H3K4me3 and H3K9me3 have opposing roles in transcription because they are correlated with active and repressed gene expression, respectively (5–9, 11). Previous chromatin immunoprecipitation-sequencing studies demonstrate that these two opposing chromatin modifications do not colocalize in the genome (15), indicating mechanisms that exclude the colocalization of these modifications. Indeed, several mechanisms have been proposed that may contribute to this exclusion (16–18, 20). Our study indicates that H3K4me3 and H3K9me3 may transiently colocalize, but in the presence of KDM4C, H3K4me3 would stimulate demethylation of H3K9me3. This mechanism of H3K4me3 stimulation could be used either to establish or maintain (previously proposed as "safeguard" (2)) active transcription. Although we hypothesize that the activity and regulation of KDM4C are crucial to the exclusion of H3K4me3 and H3K9me3, it is not known where in the genome this mechanism is required or whether it is distinct or redun-

dant with other proposed exclusion models. Due to other potentially redundant exclusion mechanisms, a precise manipulation of KDM4C activity either by a specific inhibitor or CRISPR-mediated mutation of key active site residues would be required to test its role in excluding H3K4me3 and H3K9me3 modifications.

We have uncovered a mechanism by which the interpretation of H3K4me3 by a reader TTD stimulates the removal of the repressive H3K9me3 modification through enhancing the enzymatic efficiency of KDM4C. Our work provides mechanistic insight into how KDM4C utilizes a multivalent interaction to enhance the affinity of the catalytic domain for the substrate. Moreover, our results emphasize the importance of cross-talk between chromatin modifications in generating specificity and regulating the activities of chromatin-modifying enzymes. We suggest that the coupling of the specificity of a reader domain to the enzymology of a writer or eraser can achieve and enforce distinctions between chromatin types.

Author Contributions—L. R. P., K. R. Y., and D. G. F. conceived and designed the project. L. R. P. conducted the experiments. L. R. P., K. R. Y., and D. G. F. interpreted the results and wrote the paper. All authors reviewed the results and approved the final version of the manuscript.

Acknowledgments—We thank R. Freilich and the Gestwicki laboratory for help with the isothermal titration calorimetry experiments. We thank A. Larson and G. Narlikar for advice on the in vitro pull-down experiment. We thank S. Coyle, P. Dumesic, K. Ehmsen, C. Fitzsimmons, J. Hanson, S. Isaac, M. Knuesel, A. Larson, S. Lomvardas, Y. Liu, G. Narlikar, I. Ortiz Torres, V. Stojkovic, D. Thurtle, J. Ward, C. Zhou, and members of the Fujimori and Yamamoto laboratories for helpful discussions.

References

1. Das, P. P., Shao, Z., Beyaz, S., Apostolou, E., Pinello, L., De Los Angeles, A., O'Brien, K., Atsma, J. M., Fujiwara, Y., Nguyen, M., Ljuboja, D., Guo, G., Woo, A., Yuan, G.-C., Onder, T., Daley, G., Hochedlinger, K., Kim, J., and Orkin, S. H. (2014) Distinct and combinatorial functions of Jmjd2b/Kdm4b and Jmjd2c/Kdm4c in mouse embryonic stem cell identity. *Mol. Cell* **53,** 32–48
2. Pedersen, M. T., Agger, K., Laugesen, A., Johansen, J. V., Cloos, P. A. C., Christensen, J., and Helin, K. (2014) The demethylase JMJD2C localizes to H3K4me3-positive transcription start sites and is dispensable for embryonic development. *Mol. Cell Biol.* **34,** 1031–1045
3. Martin, C., and Zhang, Y. (2005) The diverse functions of histone lysine methylation. *Nat. Rev. Mol. Cell Biol.* **6,** 838–849
4. Sanders, S. L., Portoso, M., Mata, J., Bähler, J., Allshire, R. C., and Kouzarides, T. (2004) Methylation of histone H4 lysine 20 controls recruitment of Crb2 to sites of DNA damage. *Cell* **119,** 603–614
5. Bannister, A. J., Zegerman, P., Partridge, J. F., Miska, E. A., Thomas, J. O., Allshire, R. C., and Kouzarides, T. (2001) Selective recognition of methylated lysine 9 on histone H3 by the HP1 chromo domain. *Nature* **410,** 120–124
6. Nakayama, J., Rice, J. C., Strahl, B. D., Allis, C. D., and Grewal, S. I. S. (2001) Role of histone H3 lysine 9 methylation in epigenetic control of heterochromatin assembly. *Science* **292,** 110–113
7. Grewal, S. I. S., and Jia, S. (2007) Heterochromatin revisited. *Nat. Rev. Genet.* **8,** 35–46
8. Nielsen, S. J., Schneider, R., Bauer, U.-M., Bannister, A. J., Morrison, A., O'Carroll, D., Firestein, R., Cleary, M., Jenuwein, T., Herrera, R. E., and Kouzarides, T. (2001) Rb targets histone H3 methylation and HP1 to promoters. *Nature* **412,** 561–565
9. Kouzarides, T. (2007) Chromatin modifications and their function. *Cell* **128,** 693–705
10. Bernstein, B. E., Kamal, M., Lindblad-Toh, K., Bekiranov, S., Bailey, D. K., Huebert, D. J., McMahon, S., Karlsson, E. K., Kulbokas, E. J., 3rd, Gingeras, T. R., Schreiber, S. L., and Lander, E. S. (2005) Genomic maps and comparative analysis of histone modifications in human and mouse. *Cell* **120,** 169–181
11. Santos-Rosa, H., Schneider, R., Bannister, A. J., Sherriff, J., Bernstein, B. E., Emre, N. C. T., Schreiber, S. L., Mellor, J., and Kouzarides, T. (2002) Active genes are tri-methylated at K4 of histone H3. *Nature* **419,** 407–411
12. Ng, H. H., Robert, F., Young, R. A., and Struhl, K. (2003) Targeted recruitment of Set1 histone methylase by elongating Pol II provides a localized mark and memory of recent transcriptional activity. *Mol. Cell* **11,** 709–719
13. Shilatifard, A. (2012) The COMPASS family of histone H3K4 methylases: mechanisms of regulation in development and disease pathogenesis. *Annu. Rev. Biochem.* **81,** 65–95
14. Noma, K., Allis, C. D., and Grewal, S. I. (2001) Transitions in distinct histone H3 methylation patterns at the heterochromatin domain boundaries. *Science* **293,** 1150–1155
15. Barski, A., Cuddapah, S., Cui, K., Roh, T.-Y., Schones, D. E., Wang, Z., Wei, G., Chepelev, I., and Zhao, K. (2007) High-resolution profiling of histone methylations in the human genome. *Cell* **129,** 823–837
16. Wu, H., Min, J., Lunin, V. V., Antoshenko, T., Dombrovski, L., Zeng, H., Allali-Hassani, A., Campagna-Slater, V., Vedadi, M., Arrowsmith, C. H., Plotnikov, A. N., and Schapira, M. (2010) Structural biology of human H3K9 methyltransferases. *PLoS One* **5,** e8570
17. Binda, O., LeRoy, G., Bua, D. J., Garcia, B. A., Gozani, O., and Richard, S. (2010) Trimethylation of histone H3 lysine 4 impairs methylation of histone H3 lysine 9: regulation of lysine methyltransferases by physical interaction with their substrates. *Epigenetics* **5,** 767–775
18. Shi, L., Sun, L., Li, Q., Liang, J., Yu, W., Yi, X., Yang, X., Li, Y., Han, X., Zhang, Y., Xuan, C., Yao, Z., and Shang, Y. (2011) Histone demethylase JMJD2B coordinates H3K4/H3K9 methylation and promotes hormonally responsive breast carcinogenesis. *Proc. Natl. Acad. Sci. U.S.A.* **108,** 7541–7546
19. Torres, I. O., Kuchenbecker, K. M., Nnadi, C. I., Fletterick, R. J., Kelly, M. J. S., and Fujimori, D. G. (2015) Histone demethylase KDM5A is regulated by its reader domain through a positive-feedback mechanism. *Nat Commun.* **6,** 6204
20. Horton, J. R., Upadhyay, A. K., Qi, H. H., Zhang, X., Shi, Y., and Cheng, X. (2010) Enzymatic and structural insights for substrate specificity of a family of jumonji histone lysine demethylases. *Nat. Struct. Mol. Biol.* **17,** 38–43
21. Whetstine, J. R., Nottke, A., Lan, F., Huarte, M., Smolikov, S., Chen, Z., Spooner, E., Li, E., Zhang, G., Colaiacovo, M., and Shi, Y. (2006) Reversal of histone lysine trimethylation by the JMJD2 family of histone demethylases. *Cell* **125,** 467–481
22. Klose, R. J., Yamane, K., Bae, Y., Zhang, D., Erdjument-Bromage, H., Tempst, P., Wong, J., and Zhang, Y. (2006) The transcriptional repressor JHDM3A demethylates trimethyl histone H3 lysine 9 and lysine 36. *Nature* **442,** 312–316
23. Cloos, P. A. C., Christensen, J., Agger, K., Maiolica, A., Rappsilber, J., Antal, T., Hansen, K. H., and Helin, K. (2006) The putative oncogene GASC1 demethylates tri- and dimethylated lysine 9 on histone H3. *Nature* **442,** 307–311
24. Shin, S., and Janknecht, R. (2007) Diversity within the JMJD2 histone demethylase family. *Biochem. Biophys. Res. Commun.* **353,** 973–977
25. Hillringhaus, L., Yue, W. W., Rose, N. R., Ng, S. S., Gileadi, C., Loenarz, C., Bello, S. H., Bray, J. E., Schofield, C. J., and Oppermann, U. (2011) Structural and evolutionary basis for the dual substrate selectivity of human KDM4 histone demethylase family. *J. Biol. Chem.* **286,** 41616–41625
26. Rose, N. R., McDonough, M. A., King, O. N. F., Kawamura, A., and Schofield, C. J. (2011) Inhibition of 2-oxoglutarate dependent oxygenases. *Chem. Soc. Rev.* **40,** 4364–4397
27. Johansson, C., Tumber, A., Che, K., Cain, P., Nowak, R., Gileadi, C., and Oppermann, U. (2014) The roles of Jumonji-type oxygenases in human

disease. *Epigenomics* **6,** 89–120
28. Krishnan, S., and Trievel, R. C. (2013) Structural and functional analysis of JMJD2D reveals molecular basis for site-specific demethylation among JMJD2 demethylases. *Structure* **21,** 98–108
29. Kim, J., Daniel, J., Espejo, A., Lake, A., Krishna, M., Xia, L., Zhang, Y., and Bedford, M. T. (2006) Tudor, MBT and chromo domains gauge the degree of lysine methylation. *EMBO Rep.* **7,** 397–403
30. Huang, Y., Fang, J., Bedford, M. T., Zhang, Y., and Xu, R.-M. (2006) Recognition of histone H3 lysine-4 methylation by the double tudor domain of JMJD2A. *Science* **312,** 748–751
31. Lee, J., Thompson, J. R., Botuyan, M. V., and Mer, G. (2008) Distinct binding modes specify the recognition of methylated histones H3K4 and H4K20 by JMJD2A-tudor. *Nat. Struct. Mol Biol.* **15,** 109–111
32. Mallette, F. A., Mattiroli, F., Cui, G., Young, L. C., Hendzel, M. J., Mer, G., Sixma, T. K., and Richard, S. (2012) RNF8- and RNF168-dependent degradation of KDM4A/JMJD2A triggers 53BP1 recruitment to DNA damage sites: RNF8- and RNF168-dependent degradation of KDM4A/JMJD2A. *EMBO J.* **31,** 1865–1878
33. Gibson, D. G., Young, L., Chuang, R.-Y., Venter, J. C., Hutchison, C. A., 3rd, and Smith, H. O. (2009) Enzymatic assembly of DNA molecules up to several hundred kilobases. *Nat. Methods* **6,** 343–345
34. Canzio, D., Chang, E. Y., Shankar, S., Kuchenbecker, K. M., Simon, M. D., Madhani, H. D., Narlikar, G. J., and Al-Sady, B. (2011) Chromodomain-mediated oligomerization of HP1 suggests a nucleosome-bridging mechanism for heterochromatin assembly. *Mol. Cell* **41,** 67–81
35. Couture, J.-F., Collazo, E., Ortiz-Tello, P. A., Brunzelle, J. S., and Trievel, R. C. (2007) Specificity and mechanism of JMJD2A, a trimethyllysine-specific histone demethylase. *Nat. Struct. Mol. Biol.* **14,** 689–695
36. Luger, K., Rechsteiner, T. J., and Richmond, T. J. (1999) Preparation of nucleosome core particle from recombinant histones. *Methods Enzymol.* **304,** 3–19
37. Fierz, B., Chatterjee, C., McGinty, R. K., Bar-Dagan, M., Raleigh, D. P., and Muir, T. W. (2011) Histone H2B ubiquitylation disrupts local and higher-order chromatin compaction. *Nat. Chem. Biol.* **7,** 113–119
38. Wan, Q., and Danishefsky, S. J. (2007) Free-radical-based, specific desulfurization of cysteine: a powerful advance in the synthesis of polypeptides and glycopolypeptides. *Angew. Chem. Int. Ed. Engl.* **46,** 9248–9252
39. Lowary, P. T., and Widom, J. (1998) New DNA sequence rules for high affinity binding to histone octamer and sequence-directed nucleosome positioning1. *J. Mol. Biol.* **276,** 19–42
40. Thåström, A., Bingham, L. M., and Widom, J. (2004) Nucleosomal locations of dominant DNA sequence motifs for histone-DNA interactions and nucleosome positioning. *J. Mol. Biol.* **338,** 695–709
41. Shiau, C., Trnka, M. J., Bozicevic, A., Ortiz Torres, I., Al-Sady, B., Burlingame, A. L., Narlikar, G. J., and Fujimori, D. G. (2013) Reconstitution of nucleosome demethylation and catalytic properties of a Jumonji histone demethylase. *Chem. Biol.* **20,** 494–499
42. Taverna, S. D., Li, H., Ruthenburg, A. J., Allis, C. D., and Patel, D. J. (2007) How chromatin-binding modules interpret histone modifications: lessons from professional pocket pickers. *Nat. Struct. Mol. Biol.* **14,** 1025–1040
43. Sanchez, R., and Zhou, M.-M. (2011) The PHD finger: a versatile epigenome reader. *Trends Biochem. Sci.* **36,** 364–372
44. Tong, Q., Cui, G., Botuyan, M. V., Rothbart, S. B., Hayashi, R., Musselman, C. A., Singh, N., Appella, E., Strahl, B. D., Mer, G., and Kutateladze, T. G. (2015) Structural plasticity of methyllysine recognition by the tandem tudor domain of 53BP1. *Structure* **23,** 312–321
45. Ruthenburg, A. J., Li, H., Milne, T. A., Dewell, S., McGinty, R. K., Yuen, M., Ueberheide, B., Dou, Y., Muir, T. W., Patel, D. J., and Allis, C. D. (2011) Recognition of a mononucleosomal histone modification pattern by BPTF via multivalent interactions. *Cell* **145,** 692–706
46. Ruthenburg, A. J., Allis, C. D., and Wysocka, J. (2007) Methylation of lysine 4 on histone H3: intricacy of writing and reading a single epigenetic mark. *Mol. Cell* **25,** 15–30
47. Ruthenburg, A. J., Li, H., Patel, D. J., and Allis, C. D. (2007) Multivalent engagement of chromatin modifications by linked binding modules. *Nat. Rev. Mol. Cell Biol.* **8,** 983–994
48. Lohse, B., Helgstrand, C., Kristensen, J. B. L., Leurs, U., Cloos, P. A. C., Kristensen, J. B., and Clausen, R. P. (2013) Posttranslational modifications of the histone 3 tail and their impact on the activity of histone lysine demethylases *in vitro*. *PLoS One* **8,** e67653
49. Huang, H., Sabari, B. R., Garcia, B. A., Allis, C. D., and Zhao, Y. (2014) SnapShot: histone modifications. *Cell* **159,** 458–458.e1
50. Bannister, A. J., Schneider, R., Myers, F. A., Thorne, A. W., Crane-Robinson, C., and Kouzarides, T. (2005) Spatial distribution of di- and tri-methyl lysine 36 of histone H3 at active genes. *J. Biol. Chem.* **280,** 17732–17736
51. Lin, C.-H., Li, B., Swanson, S., Zhang, Y., Florens, L., Washburn, M. P., Abmayr, S. M., and Workman, J. L. (2008) Heterochromatin protein 1a stimulates histone H3 lysine 36 demethylation by the *Drosophila* KDM4A demethylase. *Mol. Cell* **32,** 696–706
52. Bhattacharyya, R. P., Reményi, A., Yeh, B. J., and Lim, W. A. (2006) Domains, motifs, and scaffolds: the role of modular interactions in the evolution and wiring of cell signaling circuits. *Annu. Rev. Biochem.* **75,** 655–680
53. Rubenstein, E. M., and Schmidt, M. C. (2007) Mechanisms regulating the protein kinases of *Saccharomyces cerevisiae*. *Eukaryot. Cell* **6,** 571–583